Acta Biochim Biophys Sin, 2018, 50(3), 273–280
doi: 10.1093/abbs/gmy006
Advance Access Publication Date: 7 February 2018
Original Article

Original Article

MiRNA-133a is involved in the regulation of postmenopausal osteoporosis through promoting osteoclast differentiation

Zhongqi Li*, Wenzhi Zhang, and Yan Huang

Department of Orthopedics, Anhui Provincial Hospital, Hefei 230001, China

*Correspondence address. Tel: +86-551-62284089; E-mail: lizq930@sohu.com

Received 29 August 2017; Editorial Decision 18 October 2017

Abstract

The important role of miR-133a in the progress and development of postmenopausal osteoporosis has been reported, however, the underlying mechanism is not clear yet. In this study, qRT-PCR analysis was performed to assess miR-133 expression in serum isolated from postmenopausal osteoporosis patients (PMOP) and healthy controls. Bone mineral density (BMD) was measured at the lumbar spine by dual-energy X-ray absorptiometry (DXA). The results showed that miR-133a was significantly upregulated and negatively correlated with lumbar spine BMD in serum of postmenopausal osteoporotic women. The miR-133a mimic, miR-133a inhibitor, and the corresponding controls were transfected into RAW264.7 and THP-1 cells, respectively. TRAP-positive cells were counted and the protein expression of NFATc1, c-Fos and TRAP were detected by western blot analysis. We found that MiR-133a was upregulated during osteoclastogenesis, and overexpression of miR-133a promoted RANKL-induced differentiation of RAW264.7 and THP-1 cells into osteoclasts, whereas miR-133a knockdown showed the reversed results. In *in vivo* experiment, rats were bilaterally ovariectomized (OVX) and injected with antagomiR-133a or antagoNC, and were sacrificed for collecting serum and lumbar spine for ELISA, micro-computed Tomography (CT) and bone histomorphology analysis, respectively. It was found that, in OVX rats, miR-133a knockdown altered the levels of osteoclastogenesis-related factors in serum and increased lumbar spine BMD and changed bone histomorphology. Collectively, miRNA-133a is involved in the regulation of postmenopausal osteoporosis through promoting osteoclast differentiation.

Key words: miRNA-133a, postmenopausal osteoporosis, osteoclast differentiation

Introduction

Postmenopausal osteoporosis is a common bone disease characterized by low bone mineral density (BMD) and low trauma fractures caused by unbalanced bone formation by osteoblasts and bone resorption by osteoclasts [1]. It is a multifactorial disease resulting from complex interactions between genetic susceptibility and environmental factors, such as estrogen deficiency, continuous calcium loss, aging, physical activity, diet, use of certain drugs, and smoking [2,3]. Osteoporosis is a major public health concern in China that has a large aging populations [4]. Developing better treatments for patients with osteoporosis is of great importance, however, a proactive approach that identifies patients at high risk for developing osteoporosis is necessary to prevent bone loss [5,6].

MicroRNAs (miRNAs) are a superfamily of small single-stranded (about 22 nucleotides), non-coding RNAs that regulate gene expression usually by destabilizing mRNAs or by suppressing translation [6]. Numerous studies have suggested that miRNAs are important regulators associated with bone resorption by regulating proliferation and differentiation of osteoclasts, such as miR-21, miR-155, miR-223, miR-34c, and miR-378 [7–11].

© The Author(s) 2018. Published by Oxford University Press on behalf of the Institute of Biochemistry and Cell Biology, Shanghai Institutes for Biological Sciences, Chinese Academy of Sciences. All rights reserved. For permissions, please e-mail: journals.permissions@oup.com

Downloaded from https://academic.oup.com/abbs/article/50/3/273/4841916 by guest on 23 April 2024

In humans, there are two isoforms of miR-133, i.e. miR-133a and miR-133b, with one base difference (g–a) at the last nucleotide of the 3′ end (miRBase: http://www.mirbase.org/). Particularly, miR-133a was reported to be dysregulated and negatively correlated with BMD in postmenopausal osteoporosis [12,13], indicating the important role of miR-133a in the progress and development of postmenopausal osteoporosis. Wang *et al.* [12] also reported that miR-133a is a potential miRNA biomarker and/or regulatory element in circulating monocytes, which play important roles in osteoclastogenesis by acting as osteoclast precursors and secreting osteoclastogenic factors, such as interleukin (IL)−1, IL-6, and tumor necrosis factor (TNF)-α, indicating an important role of miR-133a in osteoclastogenesis.

In this study, qRT-PCR analysis was performed to assess miR-133 expression in serum isolated from postmenopausal osteoporosis patients. We found that miR-133a was significantly upregulated and negatively correlated with lumbar spine BMD in serum of postmenopausal osteoporotic women. *In vitro* experiment showed that miR-133a was upregulated during osteoclastogenesis and overexpression of miR-133a promoted RANKL-induced differentiation of RAW264.7 and THP-1 cells into osteoclasts. In addition, *in vivo* experiment showed that, in OVX rats, miR-133a knockdown altered the levels of osteoclastogenesis-related factors in serum and increased lumbar spine BMD and changed bone histomorphology. Collectively, our study indicated that miRNA-133a is involved in the regulation of postmenopausal osteoporosis through promoting osteoclast differentiation.

Methods and Materials

Clinical samples

This study was approved by the Ethics Committee of Anhui Provincial Hospital, and all human participants signed informed-consent documents. All procedures were performed in accordance with the ethical standards of the institutional and/or national research committee and with the 1964 Helsinki declaration. Ten postmenopausal Chinese women (body mass index, 23.8 ± 5.7) with osteoporosis constituted the postmenopausal osteoporosis patients (PMOP) group. All patients were past menopause at the age of 59–80 years. The recruited patients carried hip fractures (in femoral neck, trochanter, and intertrochanteric regions) that required surgical intervention. The exclusion criterias including: patients with malignancy or cancers, diabetes, cardiovascular, inflammation, and metabolic disorders as previously described [14]. Ten female participants (body mass index, 25.2 ± 3.8; age range 62–75) were used as the control group, who were randomly selected population-based sample living in the same region with the same age distribution as the patient group. Blood was collected and stored for further analysis.

Isolation of RNA from serum

Five milliliters of blood was allowed to clot, followed by centrifuging at 1500 *g*, and the supernatant containing serum was used for miRNA isolation using Qiagen miRNeasy Serum/Plasma Kit (Qiagen, Hilden, Germany) as previously described [14]. The final RNA mixture was eluted in 20 μl of RNase free water and stored at –80°C.

Quantitative real-time polymerase chain reaction (qRT-PCR)

For qRT-PCR of miR-133a, the RNA eluates were reverse transcribed to cDNA using TaqMan MicroRNA Reverse Transcription Kit (ThermoScientific, Waltham, USA) according to the manufacturer's instructions. In brief, 10 ng of total RNA was added in 1.5 μl of 10 × RT buffer, 0.15 μl of 100 mM dNTPs, 0.2 μl of 20 units/μl RNase-inhibitor, 1 μl of each of microRNA primers (100 mM), 1 μl of MultiScribe Reverse Transcriptase (50 units/μl), and 10.15 μl of DEPC treated water. The RT protocol was as follows: 18°C for 30 min, 42°C for 30 min, and 90°C for 5 min. Quantitative real-time PCR was performed on a 7900HT Fast Real-Time system (Applied Biosystems, Foster City, USA). The reaction conditions were: 95°C for 10 min, 35 cycles of 95°C for 20 s, and 58°C for 1 min. *U6* RNA was used as endogenous control for all the reactions. The relative quantity of each miRNA was determined by $2^{-\Delta\Delta CT}$ method. The primers used are listed in **Table 1**.

Bone densitometry

BMD was measured at the lumbar spine by dual-energy X-ray absorptiometry (DXA) using a Hologic 4500 bone densitometer analyzed according to WHO criteria [15].

Cell culture

The human monocytic cell line THP-1 and murine macrophage cell line RAW264.7 were purchased from the American Type Culture Collection (ATCC, Rockville, USA) and maintained in DMEM (Invitrogen, Carlsbad, USA) with 10% FBS (Invitrogen), supplemented with penicillin (100 U/ml), streptomycin (100 μg/ml) and fungizone (0.25 μg/ml). Cells were incubated at 37°C in 5% CO_2 in humidified air. For osteoclasts differentiation, RAW264.7 macrophages were cultured with 50 ng/ml macrophage colony-stimulating factor (M-CSF; Peprotech, Rocky Hill, USA) and 60 ng/ml receptor activator of nuclear factor-kappa κ ligand (RANKL; Peprotech) for 7 days.

Cell transfection

The miR-133a mimic and the negative control (miR-NC), miR-133a inhibitor (miR-133a inhibitor), and miR-133a inhibitor negative control (inhibitor-NC) were purchased from Ribobio (Guangzhou, China). The cells were transfected with 50 nM miR-133a mimic, miR-NC, miR-133a inhibitor, or inhibitor-NC by using the siPORT NeoFX transfection reagent (Ambion, Austin, USA) according to the manufacturer's instructions. After 24 h, qRT-PCR was performed to

Table 1. Primers used for qRT-PCR

Primers	Sequence
hsa-miR-133a-F	5′-CCGGGTTTGGTCCCCTTCAAC-3′
hsa-miR-133a-R	5′-GTGCAGGGTCCGAGGTCAGAGCCACCTGGGCAATTTTTTTTTTTCAGCTG-3′
mmu-miR-133a-F	5′-UUUGGUCCCCUUCAACCAGCUG-3′
mmu-miR-133a-R	5′-GTGCAGGGTCCGAGGTCAGAGCCACCTGGGCAATTTTTTTTTTTCAGCTG-3′
U6-F	5′-GTGCTCGCTTCGGCAGCACA-3′
U6-R	5′-GTGCAGGGTCCGAGGTCAGAGCCACCTGGGCAACGAATTTGCGTGTCA-3′

Downloaded from https://academic.oup.com/abbs/article/50/3/273/4841916 by guest on 23 April 2024

detect the transfection efficiency and then cultured with 50 ng/ml M-CSF and 60 ng/ml RANKL for 72 h.

Tartrate resistant acid phosphatase (TRAP)-positive cell staining

RAW264.7 or THP-1 cells (1.5×10^4 cells/well) were seeded into sterile 24-well culture plates, cells were fixed and stained using the TRAP-staining kit (Sigma-Aldrich, St Louis, USA), according to the manufacturer's instructions. TRAP-positive multinucleated cells containing more than three nuclei were counted as osteoclasts. Photomicrographs were taken with a Zeiss Axiocam MRc5 camera attached to a Zeiss Axiovert 200 microscope (Zeiss, Oberkochen, Germany).

Animal experiments

Female Wistar rats weighing 205 ± 8 g were purchased from the animal laboratory of the Chinese Academy of Medical Science (Beijing, China). The rats were kept together for 2 weeks to acclimatize, fed with commercially available feed, and had access to feed and water *ad libitum*. All of the rats were kept under controlled lighting (light: dark, 12:12 h) and temperature (22 ± 1°C) conditions. The study was approved by the Ethics Committee of Anhui Provincial Hospital. At 6 months of age, 30 rats were starved for 12 h at first stage and then were bilaterally ovariectomized (OVX) under 25 mg/kg thiopental sodium anesthesia as described previously [16]. These rats were then divided in to three groups: OVX, OVX rats injected with antago-NC (antago-NC group), and OVX rats injected with antagomiR-133a (antagomiR-133a group). The OVX rats received distilled water was used as the control (Sham group, $n = 10$). These rats received either antagomiR-133a (10 nmol/per mouse) or antago-NC (RiboBio Co, Guangzhou, China) through tail vein injection on Days 1 to 3 for 3 consecutive weeks. Three weeks after the last injection, rats were euthanized and blood was taken by dorsal aortic puncture. Rats were euthanized for collecting serum and lumbar spine for ELISA and micro-computed Tomography (CT) analysis, respectively. The levels of M-CSF, RANKL, tumor necrosis factor (TNF)-α, interleukin (IL)-1α, C-terminal telopeptide of type-I collagen (CTX-I), and bone Gla-protein (BGP) in serum were measured using enzyme-linked immunosorbent assay kits (R&D Systems, Minneapolis, USA). The micro-CT analysis was performed as described previously [17].

Bone histomorphometry

At sacrifice of rats, the lumbar spine was fixed with 10% formalin and was cut at the midshaft using a rotary electronic saw (Black & Decker, Towson, USA). The distal tibias were then halved longitudinally and dehydrated in ethanol, and then embedded in methyl methacrylate polymer according to the manufacturer's instructions (Osteo-Bed Bone Embedding Kit; Polysciences Inc., Warrington, USA). Then, the tibias were sectioned using a Manual Rotary Microtome (Model 2235; Leica, Solms, Germany) and 7 μm thick serial bone section was obtained. Measurements were made at 4× objective magnification using a light microscope (Leica) connected to an image analyzer (Image Pro-Express; Bethesda, USA). Static parameters of bone tissue morphology including bone volume/total volume (BV/TV, %), trabecular thickness (Tb.Th, mm) and trabecular number (Tb.N, mm^{-1}) were calculated as previously described [18,19].

Western blot analysis

Protein was collected from lumbar spine and lysed in radioimmunoprecipitation buffer (RIPA) containing protease inhibitors at 4°C for 30 min. Cell lysates were prepared with RIPA lysis buffer kit (Santa Cruz Biotech, Santa Cruz, USA), and the protein concentrations were quantified using a Bio-Rad protein assay (Bio-Rad, Hercules, USA). Proteins (30 μg) were separated by 8% SDS-PAGE and transferred to polyvinylidene difluoride membranes (Amersham, Chicago, USA). The membranes were blocked with 5% non-fat milk (Merck, San Diego, USA) overnight at 4°C. Then membranes were incubated with the following primary antibodies: anti-NFATc1 antibody (1:20; Invitrogen), anti-c-Fos antibody (1:2000; Abcam, Chicago, USA), anti-TRAP antibody (1:2000; Abcam), and anti-β-actin antibody (1:2000; Abcam) overnight at 4°C. After extensive wash, membranes were incubated with a horseradish peroxidase-conjugated secondary antibody (1:1000; Beijing Zhongshan Golden Bridge Biotechnology Co, Beijing, China) at room temperature for 1 h. Finally, signals were detected using an enhanced chemiluminescence kit (Wuhan Booute Biotechnology Co, Wuhan, China) and exposed to Kodak X-OMAT film (Kodak, Rochester, USA).

Statistical analysis

Data were expressed as the mean ± standard deviation (SD). Each experiment was performed at least three times. The comparisons

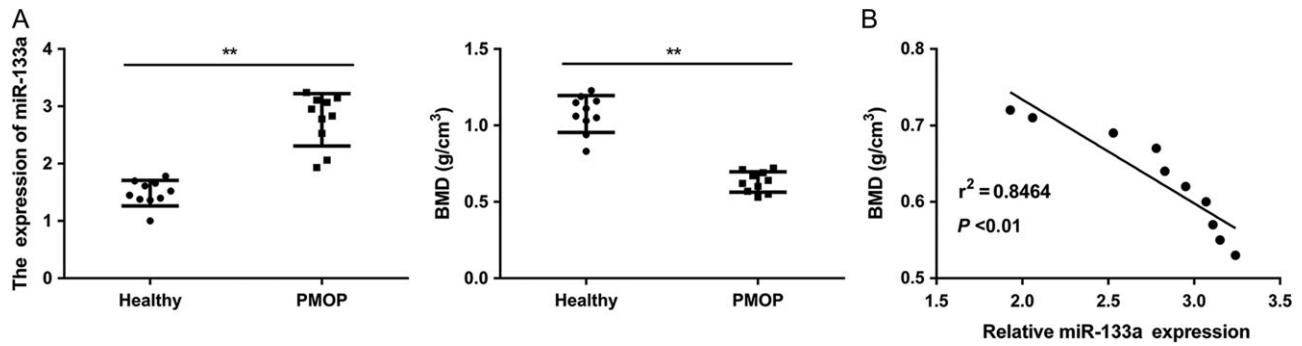

Figure 1. MiR-133a is significantly upregulated and negatively correlated with lumbar BMD in serum of postmenopausal osteoporotic women (A) the expression of miR-133a in serum and BMD in the postmenopausal osteoporotic group and healthy control group. (B) Spearman correlation analysis between miR-133a expression and lumbar BMD in postmenopausal osteoporotic group. $n = 10$ in each group. Blood was collected for analysis of miR-133a expression. BMD was measured at the lumbar by DXA. PMOP group, postmenopausal osteoporotic women. Healthy group, the control healthy women. $^{**}P < 0.01$ compared with the healthy group.

Downloaded from https://academic.oup.com/abbs/article/50/3/273/4841916 by guest on 23 April 2024

between two groups were performed using the independent Student's *t*-test. For comparisons among three or more groups, one-way ANOVA with Tukey *post hoc* test was used. Spearman correlations analysis was performed to examine the relationship between miR-133a expression level and lumbar BMD. The statistical significance was set at $P < 0.05$. The SPSS 15.0 statistical software (SPSS Inc., Chicago, USA) was used for all statistical analyses.

Results

MiR-133a is significantly upregulated and negatively correlated with lumbar spine BMD in serum of postmenopausal osteoporotic women

As shown in **Fig. 1A**, the expression of miR-133a was significantly upregulated in serum of postmenopausal osteoporotic women (PMOP group, $n = 10$, $P < 0.01$) as compared with the control healthy group (Healthy group, $n = 10$). However, the BMD was significantly lower in PMOP group as compared with the healthy group. The Spearman correlations analysis (**Fig. 1B**) showed that negative correlation existed between miR-133a expression and lumbar BMD in postmenopausal osteoporotic women (PMOP group, $n = 10$; $P < 0.01$, $r^2 = 0.8464$).

Overexpression of miR-133a promotes RANKL-induced differentiation of RAW264.7 and THP-1 cells into osteoclasts

To determine whether the expression of miR-133a is altered during osteoclastogenesis in RAW264.7 and THP-1 cells, qRT-PCR was performed. RAW264.7 and THP-1 cells were treated with RANKL (60 ng/ml) and M-CSF (50 ng/ml) for 7 days. As shown in **Fig. 2A**, miR-133a was upregulated in RANKL/M-CSF-induced RAW264.7 and THP-1 cells in a time-dependent manner, indicating that miR-133a was upregulated during osteoclastogenesis.

To explore the role of miR-133a in osteoclastogenesis, RAW264.7 and THP-1 cells were transfected with miR-133a mimic and the negative control (miR-NC), respectively. RAW264.7 and THP-1 cells were then treated with RANKL (60 ng/ml) and M-CSF (50 ng/ml) for 72 h. The qRT-PCR results showed that miR-133a mimic was successfully transfected into RAW264.7 and THP-1 cells (**Fig. 2B**).

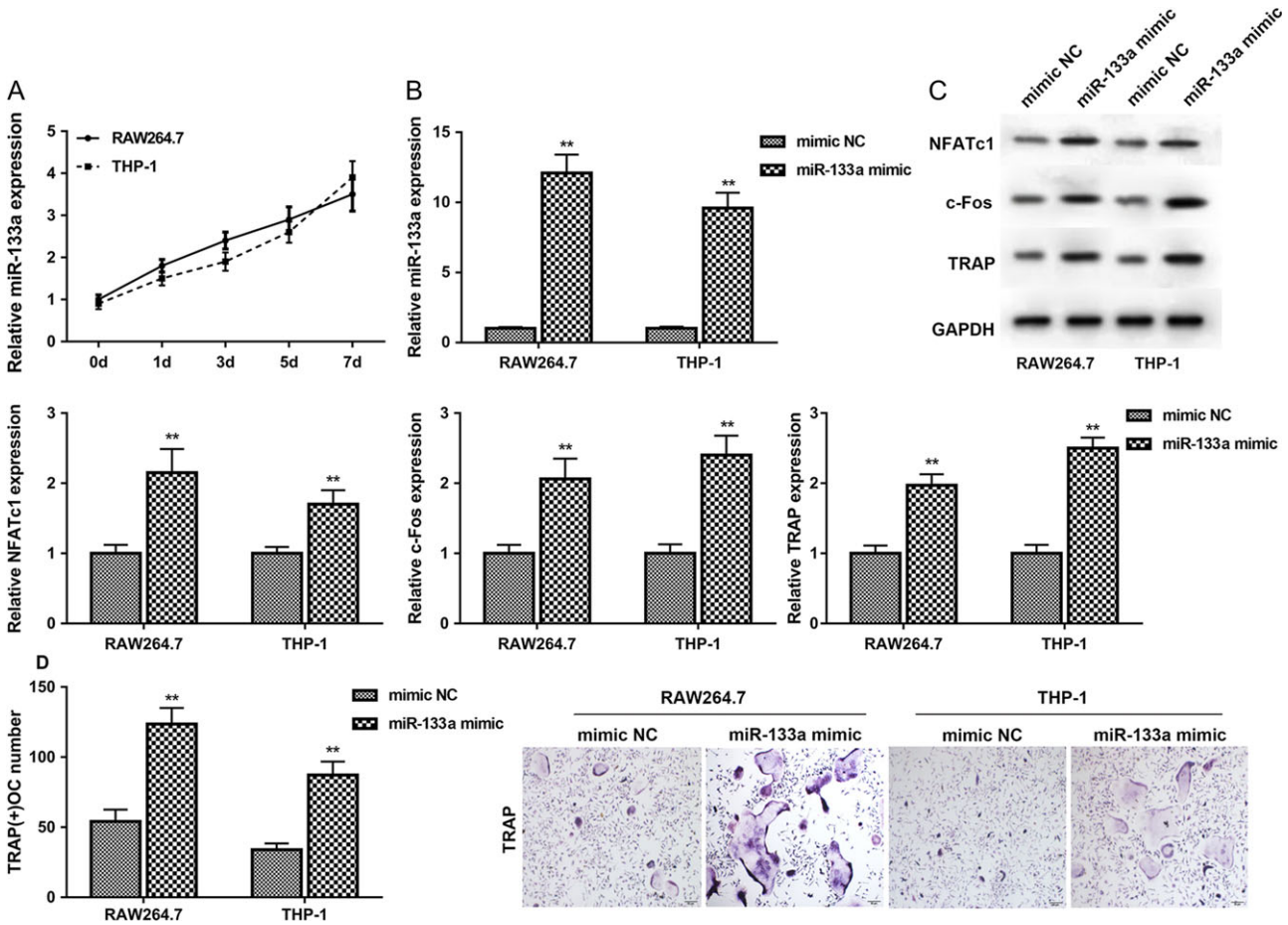

Figure 2. Overexpression of miR-133a promotes RANKL-induced differentiation of RAW264.7 and THP-1 cells into osteoclasts (A) The expression of miR-133a in RANKL/M-CSF-induced RAW264.7 and THP-1 cells. RAW264.7 and THP-1 cells were treated with RANKL (60 ng/ml) and M-CSF (50 ng/ml) for 7 days, followed by qRT-PCR analysis. (B) miR-133a mimic was successfully transfected into RAW264.7 and THP-1 cells. (C) The protein expression levels of NFATc1, c-Fos and TRAP in miR-133a mimic and miR-NC groups. (D) The number of TRAP-positive cells in miR-133a mimic and miR-NC groups. RAW264.7 and THP-1 cells were transfected with miR-133a mimic and the negative control (miR-NC), respectively. RAW264.7 and THP-1 cells were then treated with RANKL (60 ng/ml) and M-CSF (50 ng/ml) for 72 h. qRT-PCR analysis was used to detect the expression of miR-133a, and western blot analysis was used to detect the protein levels of NFATc1, c-Fos and TRAP. TRAP-positive multinucleated cells containing more than three nuclei were counted as osteoclasts. $^{**}P < 0.01$ compared with the miR-NC group.

Downloaded from https://academic.oup.com/abbs/article/50/3/273/4841916 by guest on 23 April 2024

It was found that the protein expression levels of NFATc1, c-Fos, and TRAP were significantly increased in the miR-133a mimic group as compared with the miR-NC group (**Fig. 2C**; $P < 0.01$). In addition, it was also found that TRAP-positive cells in miR-133a mimic group were significantly increased as compared with the miR-NC group (**Fig. 2D**; $P < 0.01$). These results indicated that miR-133a was upregulated during osteoclastogenesis and overexpression of miR-133a promoted RANKL-induced differentiation of RAW264.7 and THP-1 cells into osteoclasts.

MiR-133a knockdown inhibits RANKL-induced differentiation of RAW264.7 and THP-1 cells into osteoclasts

RAW264.7 and THP-1 cells were also transfected with miR-133a inhibitor (miR-133a inhibitor), and miR-133a inhibitor negative control (inhibitor-NC), respectively. RAW264.7 and THP-1 cells were then treated with RANKL (60 ng/ml) and M-CSF (50 ng/ml) for 72 h. The qRT-PCR results showed that miR-133a inhibitor was successfully transfected into RAW264.7 and THP-1 cells (**Fig. 3A**). Indeed, we found that the protein expression levels of NFATc1, c-Fos and TRAP were significantly decreased in miR-133a inhibitor group as compared with the inhibitor-NC group (**Fig. 3B**; $P < 0.01$). It was also found that TRAP-positive cells in miR-133a inhibitor group were significantly decreased as compared with the inhibitor-NC group (**Fig. 3C**; $P < 0.01$). These results indicated that miR-133a knockdown inhibited RANKL-induced differentiation of RAW264.7 and THP-1 cells into osteoclasts.

MiR-133a knockdown alters the levels of osteoclastogenesis-related factors in serum of OVX rats

miR-133a was successfully knocked down in OVX rats after infecting with antagomiR-133a (**Fig. 4A**; $P < 0.01$). It was found that miR-133a knockdown (antagomiR-133a) significantly decreased the serum levels of M-CSF (**Fig. 4B**; $P < 0.01$), RANKL (**Fig. 4B**; $P < 0.01$), TNF-α (**Fig. 4C**; $P < 0.05$), IL-1α (**Fig. 4C**; $P < 0.01$), and CTX-I (**Fig. 4D**;

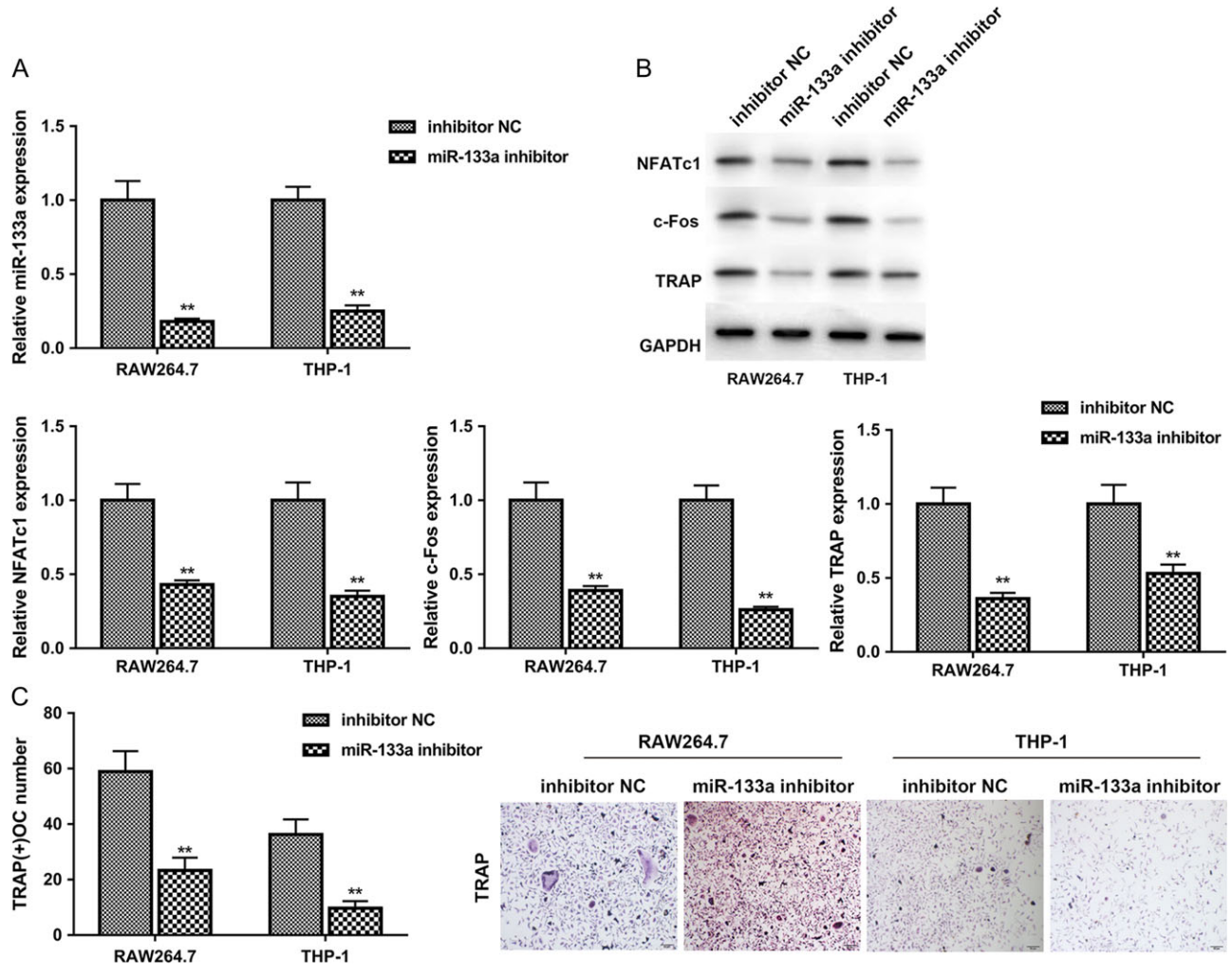

Figure 3. MiR-133a knockdown inhibits RANKL-induced differentiation of RAW264.7 and THP-1 cells into osteoclasts (A) miR-133a inhibitor was successfully transfected into RAW264.7 and THP-1 cells. (B) The protein expression levels of NFATc1, c-Fos, and TRAP in miR-133a inhibitor and inhibitor-NC groups. (C) The number of TRAP-positive cells in miR-133a inhibitor and inhibitor-NC groups. RAW264.7 and THP-1 cells were transfected with miR-133a inhibitor and inhibitor-NC. RAW264.7 and THP-1 cells were then treated with RANKL (60 ng/ml) and M-CSF (50 ng/ml) for 72 h. qRT-PCR analysis was used to detect the expression of miR-133a, and western blot analysis was used to detect the protein levels of NFATc1, c-Fos and TRAP. TRAP-positive multinucleated cells containing more than three nuclei were counted as osteoclasts. $^{**}P < 0.01$ compared with the inhibitor NC group.

Downloaded from https://academic.oup.com/abbs/article/50/3/273/4841916 by guest on 23 April 2024

$P < 0.05$), but markedly increased the serum level of BGP (**Fig. 4D**; $P < 0.05$) in OVX rats as compared with control (**Fig. 4**).

MiR-133a knockdown increases lumbar spine BMD and changes bone histomorphology in OVX rats

As shown in **Fig. 5A**, miR-133a knockdown (antagomiR-133a) significantly increased lumbar spine BMD in OVX rats as compared with the control ($P < 0.01$). The 2D micro-CT image also showed that OVX-induced bone destruction was notably reduced by antagomiR-133a (**Fig. 5B**). Histomorphometry is an important technique for examining bone quality and architecture, and is used diagnostically in metabolic bone diseases such as osteoporosis As shown in **Fig. 5C**, osteoporosis rat induced by OVX had a reduced BV/TV, Tb.Th, and Tb.N compared with the Sham group. Treatment with antagomiR-133a significantly prevented these reductions. To sum up, the significantly low BV/TV, Tb.Th, and Tb.N in OVX rats were clear evidence of bone loss, mainly due to trabecular perforation, trabecular thinning and loss of trabecular connectivity, and they were all attenuated by treatment with antagomiR-133a.

Discussion

In our study, miR-133a was found to be significantly upregulated and negatively correlated with lumbar spine BMD in serum of postmenopausal osteoporotic women. Consistently, miR-133a was reported to be dysregulated and negatively correlated with BMD in postmenopausal osteoporosis [12,13]. MiR-133a was also found to regulate osteoblastogenesis by targeting and regulating Runx2 expression [20]. In osteoblast cell line MC3T3, overexpressed miR133a directly targets the *Runx2* gene 3′-UTR, which suppresses alkaline phosphatase production and osteoblast differentiation [20]. Zhou *et al.* [21] demonstrated that miR-133a was upregulated in osteoblast-like periodontal ligament stem cells treated with ibandronate, a nitrogen-containing bisphosphonate that is widely used to treat osteoporosis and inhibits bone resorption. Lv *et al.* [22] showed that estrogen deficiency is associated with miR-133 overexpression and miR-133 can induce postmenopausal osteoporosis by weakening osteogenic differentiation of human mesenchymal stem cells, at least partly through repressing SLC39A1 expression.

In vitro experiment showed that miR-133a was upregulated in RANKL/M-CSF-induced RAW264.7 and THP-1 cells in a time-dependent manner, indicating that miR-133a was upregulated during osteoclastogenesis. In addition, overexpression of miR-133a significantly increased the protein expression of NFATc1, c-Fos, and TRAP and significantly increased the number of TRAP-positive cells in RANKL-treated RAW264.7 and THP-1 cells. On the contrary, miR-133a knockdown showed the contrary results. Osteoclasts cells are primarily responsible for bone resorption, and osteoclasts differentiation is modulated by various processes through differential gene expression [23]. It is well-known that RANKL stimulation triggers the recruitment of tumor necrosis factor receptor-associated factor 6 (TRAF6), resulting in the activation of downstream transcription factors including c-Fos and NFATc1, and thereby leading to the increased expression of TRAP [24]. Then, many osteoclastogenesis-related marker genes, such as TRAP, MMP-9, and cathepsin K are activated [25]. NFATc1-deficient embryonic stem cells fail to differentiate into osteoclasts, and ectopic expression of NFATc1 causes precursor cells to undergo efficient differentiation without RANKL stimulation [26]. Mice lacking c-Fos develop osteoporosis as a result of a complete ablation of osteoclast formation [27]. Thus, it proves that miR-133a plays an important role in RANKL-induced differentiation of RAW264.7 and THP-1 cells into osteoclasts.

Biochemical markers of bone resorption and formation are sensitive markers that reflect the different processes involved in bone metabolism. M-CSF, RANKL, TNF-α, IL-1α, CTX-I, and BGP are well-accepted as osteoclastogenesis-related factors. M-CSF or RANKL are two key cytokines involved in osteoclast development [28]. Inflammatory cytokines TNF-α and IL-1α have been shown to contribute to osteoclastogenesis [28,29]. CTX-I is known as a specific

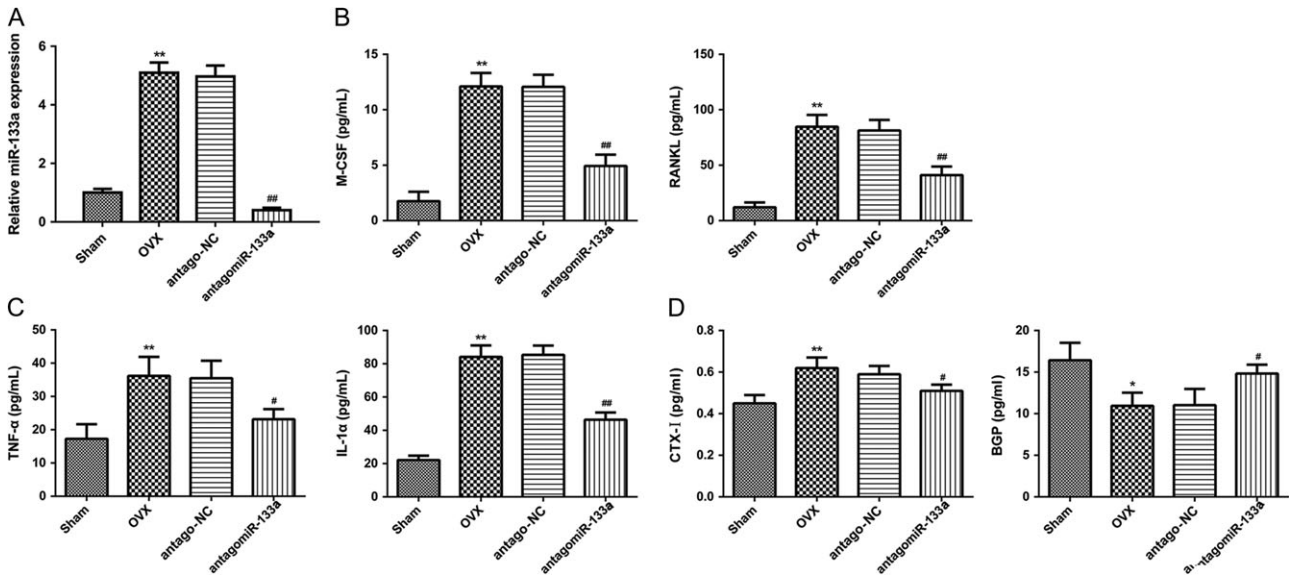

Figure 4. MiR-133a knockdown alters the levels of osteoclastogenesis-related factors in serum of OVX rats (A) MiR-133a was successfully knocked down in OVX rats. The serum levels of M-CSF (B), RANKL (B), TNF-α (C), IL-1α (C) and CTX-I (D) and BGP (D) in Sham, OVX, antago-NC and antagomiR-133a groups. $n = 10$ in each group. $^{*}P < 0.05$ and $^{**}P < 0.01$ compared with the Sham group. $^{\#}P < 0.05$ and $^{\#\#}P < 0.01$ compared with the antago-NC group. The levels of M-CSF, RANKL, TNF-α, IL-1α, CTX-I, and BGP in serum were measured by ELISA.

Downloaded from https://academic.oup.com/abbs/article/50/3/273/4841916 by guest on 23 April 2024

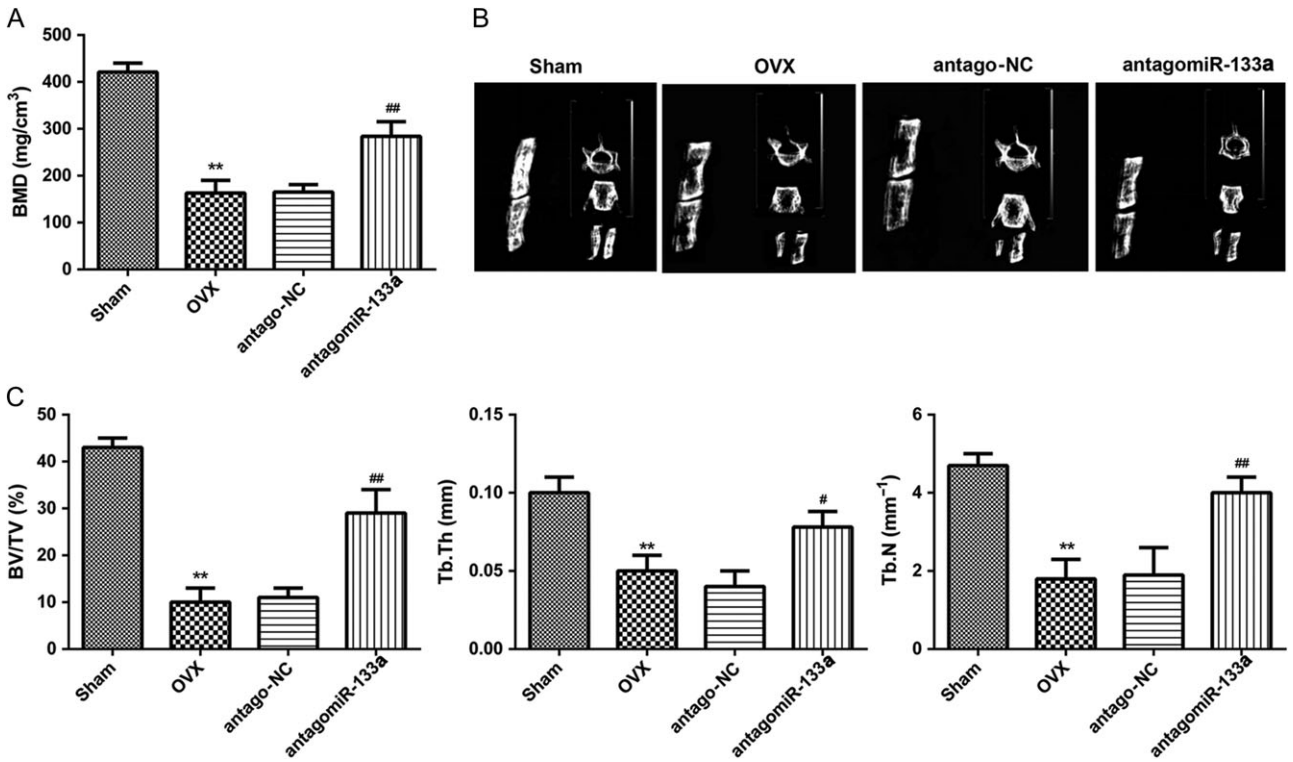

Figure 5. MiR-133a knockdown increases lumbar spine BMD and changes bone histomorphology in OVX rats (A) The lumbar spine BMD in Sham, OVX, antago-NC, and antagomiR-133a groups. BMD was measured at the lumbar by DXA. (B) The 2D micro-CT images in Sham, OVX, antago-NC, and antagomiR-133a groups. (C) The histomorphometry analysis in Sham, OVX, antago-NC, and antagomiR-133a groups. $n = 10$ in each group. $^{*}P < 0.05$ and $^{**}P < 0.01$ compared with the Sham group. $^{\#}P < 0.05$ and $^{\#\#}P < 0.01$ compared with the antago-NC group.

marker for osteoclast activity and bone resorption [30], and BGP, also called osteocalcin, forms about 10% of noncollagenous proteins of the bone matrix and generally serves as a specific marker for osteoblast activity and bone formation [31]. *In vivo* experiment showed that, in OVX rats, miR-133a knockdown altered the levels of osteoclastogenesis-related factors M-CSF, RANKL, TNF-α, IL-1α, CTX-I, and BGP in serum, increased lumbar spine BMD, and changed bone histomorphology. Osteotropic agents, such as IL-1 and TNF-α, could result in bone loss by increasing osteoclast formation [32,33]. The results of bone histomorphology analysis showed that the loss of bone in OVX rats was mainly due to trabecular perforation and loss of trabecular connectivity and trabecular thinning [34]. Trabecular perforation may therefore lead to an increased bone fragility [35] associated with an increase in systemic bone turnover markers at the tissue level [36]. Importantly, miR-133a knockdown in OVX rats completely prevented the bone loss. These results showed that miR-133a plays an important role in bone loss by altering the serum levels of osteoclastogenesis-related factors, decreasing lumbar spine BMD, and changing bone histomorphology.

To sum up, our results showed that miR-133a was significantly upregulated and negatively correlated with lumbar spine BMD in serum of postmenopausal osteoporotic women. MiR-133a was upregulated during osteoclastogenesis and promoted RANKL-induced differentiation of RAW264.7 and THP-1 cells into osteoclasts *in vitro*. MiR-133a also plays an important role in bone loss by altering the serum levels of osteoclastogenesis-related factors, decreasing lumbar spine BMD and changing bone histomorphology *in vivo*. Taken together, miRNA-133a is involved in the regulation of postmenopausal osteoporosis through promoting osteoclast differentiation.

References

1. Kida S. The unitary model for estrogen deficiency and the pathogenesis of osteoporosis: is a revision needed? *J Bone Miner Res* 2011, 26: 441.
2. Kanis JA, Burlet N, Cooper C, Delmas PD, Reginster JY, Borgstrom F, Rizzoli R. European guidance for the diagnosis and management of osteoporosis in postmenopausal women. *Osteoporos Int* 2008, 19: 399–428.
3. Jia M, Zhang D, Pan N, Ning S, Wang Q, Fan J, Ping Z, *et al*. Identification of miR-194-5p as a potential biomarker for postmenopausal osteoporosis. *Peer J* 2015, 3: e971.
4. Feng Z, Liu C, Guan X, Mor V. China's rapidly aging population creates policy challenges in shaping a viable long-term care system. *Health Aff (Millwood)* 2012, 31: 2764.
5. Sanders S, Geraci SA. Osteoporosis in postmenopausal women: considerations in prevention and treatment: (women's health series). *South Med J* 2013, 106: 698–706.
6. Tella SH, Gallagher JC. Prevention and treatment of postmenopausal osteoporosis. *J Steroid Biochem* 2014, 142: 155.
7. Sugatani T, Vacher J, Hruska KA. A microRNA expression signature of osteoclastogenesis. *Blood* 2011, 117: 3648.
8. Mizoguchi F, Izu Y, Hayata T, Hemmi H, Nakashima K, Nakamura T, Kato S, *et al*. Osteoclast-specific Dicer gene deficiency suppresses osteoclastic bone resorption. *J Cell Biochem* 2010, 109: 866–875.
9. Sugatani T, Hruska KA. Impaired micro-RNA pathways diminish osteoclast differentiation and function. *J Biol Chem* 2009, 284: 4667.
10. Bae Y, Yang T, Zeng HC, Campeau PM, Chen Y, Bertin T, Dawson BC, *et al*. miRNA-34c regulates Notch signaling during bone development. *Hum Mol Genet* 2012, 21: 2991.
11. Kagiya T, Nakamura S. Expression profiling of microRNAs in RAW264.7 cells treated with a combination of tumor necrosis factor alpha and RANKL during osteoclast differentiation. *J Periodontal Res* 2013, 48: 373.

Downloaded from https://academic.oup.com/abbs/article/50/3/273/4841916 by guest on 23 April 2024

12. Wang Y, Li L, Moore BT, Peng XH, Fang X, Lappe JM, Recker RR, *et al*. MiR-133a in human circulating monocytes: A potential biomarker associated with postmenopausal osteoporosis. *PLoS One* 2012, 7: e34641.
13. Li H, Wang Z, Fu Q, Zhang J. Plasma miRNA levels correlate with sensitivity to bone mineral density in postmenopausal osteoporosis patients. *Biomarkers* 2014, 19: 553.
14. Chen H, Jiang H, Dan C, Xu H, Zhang K, Guo S. Evaluation of MicroRNA 125b as a potential biomarker for postmenopausal osteoporosis. *Trop J Pharm Res* 2017, 16: 641.
15. Organization WH. Assessment of fracture risk and its application to screening for postmenopausal osteoporosis. *World Health Organ Tech Rep Ser* 1994, 843: 1–129.
16. Kalu DN. The ovariectomized rat model of postmenopausal bone loss. *Bone Miner* 1991, 15: 175.
17. Cuellar JM, Yoo A, Tovar N, Coelho PG, Jimbo R, Vandeweghe S, Kirsch T, *et al*. The effects of Amicar and TXA on lumbar spine fusion in an animal model. *Spine* 2014, 39: E1132.
18. Lin JT, Tie WU, Cui L, Qiong YU, Guo Z, Chen ZD. The effect of YPF extract on morphometry of bone in model rats with osteoporosis which induced by cyclophosphamide. *Liaoning J Tradit Chin Med* 2007, 8: 1159–1161.
19. Baron R, Vignery A, Neff L, Silverglate A, Maria AS, Baron R, Vignery A, *et al*. Processing of undecalcified bone specimens for bone histomorphometry. *Bone Histomorphometry Teachniques & Interpretation* 1983.
20. Zhang Y, Xie RL, Croce CM, Stein JL, Lian JB, van Wijnen AJ, Stein GS. A program of microRNAs controls osteogenic lineage progression by targeting transcription factor Runx2. *Proc Natl Acad Sci USA* 2011, 108: 9863–9868.
21. Zhou Q, Zhao ZN, Cheng JT, Zhang B, Xu J, Huang F, Zhao RN, *et al*. Ibandronate promotes osteogenic differentiation of periodontal ligament stem cells by regulating the expression of microRNAs. *Biochem Biophys Res Commun* 2011, 404: 127–132.
22. Lv H, Sun Y, Zhang Y. MiR-133 is involved in estrogen deficiency-induced osteoporosis through modulating osteogenic differentiation of mesenchymal stem cells. *Med Sci Monit* 2014, 21: 1527–1534.
23. Lee EG, Yun HJ, Lee SI, Yoo WH. Ethyl acetate fraction from *Cudrania tricuspidata* inhibits IL-1β-stimulated osteoclast differentiation through downregulation of MAPKs, c-Fos and NFATc1. *Korean J Intern Med* 2010, 25: 93–100.
24. Teitelbaum SL, Ross FP. Genetic regulation of osteoclast development and function. *Nat Rev Gene* 2003, 4: 638–649.
25. Wei ZF, Tong B, Xia YF, Lu Q, Chou GX, Wang ZT, Dai Y. Norisoboldine suppresses osteoclast differentiation through preventing the accumulation of TRAF6-TAK1 complexes and activation of MAPKs/NF-κB/c-Fos/NFATc1 pathways. *PLoS One* 2013, 8: e59171.
26. Sharma SM, Agnieszka B, Rong H, Krupen P, Mansky KC, Said S, Ostrowski MC. MITF and PU.1 recruit p38 MAPK and NFATc1 to target genes during osteoclast differentiation. *J Biol Chem* 2007, 282: 15921–15929.
27. Cheng B, Li J, Du J, Xiang L, Li W, Ling C. Ginsenoside Rb1 inhibits osteoclastogenesis by modulating NF-κB and MAPKs pathways. *Food Chem Toxicol* 2012, 50: 1610–1615.
28. Harvey BP, Syed F, Kaymakcalan Z. THU0028 Fibroblast-like synoviocytes inhibit TNF- and RANKL-induced human osteoclast precursor differentiation following exposure to IL-1BETA. *Ann Rheum Dis* 2012, 71: 162–163.
29. Ma T, Miyanishi K, Suen A, Epstein NJ, Tomita T, Smith RL, Goodman SB. Human interleukin-1-induced murine osteoclastogenesis is dependent on RANKL, but independent of TNF-alpha. *Cytokine* 2004, 26: 138–144.
30. Vasikaran SD. Utility of biochemical markers of bone turnover and bone mineral density in management of osteoporosis. *Crit Rev Clin Lab Sci* 2008, 45: 221–258.
31. Dogan E, Posaci C. Monitoring hormone replacement therapy by biochemical markers of bone metabolism in menopausal women. *Postgrad Med J* 2002, 78: 727–731.
32. Suda T, Takahashi N, Jimi N, Gillespie E, Martin M.T. Modulation of osteoclast differentiation and function by the new members of the tumor necrosis factor receptor and ligand families. *Endocr Rev* 1999, 20: 345–357.
33. Hofbauer LC, Sundeep K, Dunstan CR, Lacey DL, Boyle WJ, Lawrence RB. The roles of osteoprotegerin and osteoprotegerin ligand in the paracrine regulation of bone resorption. *J Bone Miner Res* 2000, 15: 2–12.
34. Compston JE, Croucher PI. Histomorphometric assessment of trabecular bone remodelling in osteoporosis. *Bone Miner* 1991, 14: 91–102.
35. Peel N. Bone remodelling and disorders of bone metabolism. *Surgery* 2009, 27: 70–74.
36. Tanaka M, Mori H, Kayasuga R, Ochi Y, Kawada N, Yamada H, Kishikawa K. Long-term minodronic acid (ONO-5920/YM529) treatment suppresses increased bone turnover, plus prevents reduction in bone mass and bone strength in ovariectomized rats with established osteopenia. *Bone* 2008, 43: 894–900.

Downloaded from https://academic.oup.com/abbs/article/50/3/273/4841916 by guest on 23 April 2024